

Electronic Supplementary Information

Pt embedded in carbon rods of N-doped CMK-3 as highly active and stable catalyst for catalytic hydrogenation reduction of bromate

Minghui Li, Yuan Hu, Heyuan Fu, Xiaolei Qu, Zhaoyi Xu, Shourong Zheng*

State Key Laboratory of Pollution Control and Resource Reuse, Jiangsu Key Laboratory of Vehicle Emissions Control, School of the Environment, Nanjing University, Nanjing 210093, PR China

Table of Contents

Experimental Section	Pages 2-5
Supplementary Figures	Pages 6-16
Supplementary Table	Page 17-18
Calculation	Page 19
References	Page 20-21

Experimental Section

Materials and reagents

Absolute ethanol (analytical reagent grade), tetraethoxysilane (TEOS), triblock copolymer Pluronic P123 (EO20PO70EO20) with average 5,800 molecular weight and hydrogen hexachloroplatinate (IV) hexahydrate ($\text{H}_2\text{PtCl}_6 \cdot 6\text{H}_2\text{O}$) was purchased from Aldrich. Hydrogenchloride (HCl), hydrogenfluoride (HF), furfuryl alcohol (FA), oxalic acid (OA), 1,3,5-trimethylbenzene(TMB), AlCl_3 and quinolone were obtained from Merck. Glucose (Analytical-grade) was purchased from Sinopharm Chemical Reagent Co., Ltd. Commercial Pt(1.0)/C catalyst was purchased from Alfa Aesar (China). Distilled deionized water was used in the experiments. All chemicals were used without further purification.

Pristine CNT with a diameter of 40-60 nm and a length of 5-15 μm was supplied by Shenzhen Nanotech Port Co., Ltd. (China). The CNT was pretreated to remove amorphous carbon and trace metals using a method described in previous studies.^{1,2}

Preparation of SBA-15

The mesoporous silica SBA-15 was synthesized according to the procedure described by Zhao et al.³ Briefly, 8.0 g of P123 was added to a solution containing 240 ml HCl (2 mol l^{-1}) and 60 ml distilled water. This mixed solution was subjected to continuous stirring at 40 °C for 4 h. Then, 18 g of TEOS was slowly added. The resultant mixture was transferred to Teflon-lined autoclaves and heated at 100 °C for 48 h. The mesoporous silica was obtained by filtration, followed by washing with distilled water, drying at 80 °C and calcining at 550 °C in air for 6 h to remove the surfactant.

Preparation of aluminosilicate template (Al-SBA-15)

Calcined SBA-15 was dispersed in an ethanol solution of AlCl_3 (with a molar ratio of Si/Al = 20). After the ethanol was completely evaporated at room temperature, the

samples were dried at 90 °C and calcined in air at 550 °C for 2 h. After cooled down to room temperature, the resultant Al-SBA-15 sample was stored for further use.

Preparation of SBA-15 with hollow carbon tubes composite

The synthesis of SBA-15 with hollow carbon tubes composite was conducted according to a reported procedure.⁴ FA was incorporated into the channel of Al-SBA-15 by incipient wetness infiltration. Then, the mixture was placed in the oven at 80 °C for 16 h and then at 150 °C for 6 h. The resulting dark-brown solid sample was washed with EtOH and acetone until colorless, and further carbonized under nitrogen atmosphere in a quartz tube furnace by ramping from room temperature to 850 °C at a heating rate of 5 °C min⁻¹ and holding at 850 °C for 3 h.

Preparation of SBA-15 with hollow N-doped carbon tubes composite

SBA-15 with hollow N-doped carbon tubes was prepared using a N-containing polymer as a carbon precursor. Particularly, poly-quinoline was used a suitable choice due to its gentle polymerization reaction among N-containing polymers.⁵ According to previously reported methods, Al-SBA-15 (1 g) was infiltrated with quinolone (1 ml), and introduced into an autoclave under an N₂ atmosphere for maturation at 250 °C for 12 h. Finally, the obtained dark-brown material was transferred to a quartz tube and carbonized at 850 °C for 4 h under N₂ atmosphere.

Preparation of embedded Pt catalyst

The preparation of the embedded Pt catalyst was carried out by incipient wetness impregnation in two consecutive steps.^{6,7} Briefly, 1 g grinded and sieved SBA-15 with hollow carbon and/or N-doped tubes composite was impregnated with an equal pore volume aqueous solution containing a desired amount of H₂PtCl₆. After mixed well by stirring, the humid samples were oven-dried at 105 °C for overnight, calcined in a tubular furnace with a heating rate of 5 °C min⁻¹ up to 500 °C and maintained this temperature for 5 h at N₂ atmosphere. To embed Pt particles into carbon rods, FA was infiltrated into the pore according to the reported method.⁸ FA was dissolved in TMB

in a 40/60 volume ratio and OA was added to this solution (FA: TMB: OA mole ratio of 200:185:1). The resulting solution was infiltrated into the sample. After completely mixing, the mixture was placed in the oven at 80 °C for 16 h and then at 150 °C for 6 h. The resulting dark-brown solid sample was carbonized under N₂ atmosphere in a furnace by ramping from room temperature to 300 °C at a heating rate of 1 °C min⁻¹. Then the temperature was increased to 850 °C at a heating rate of 5 °C min⁻¹ and kept at this temperature for 4 h. Finally, the silica template was selectively removed using an aqueous 10% HF solution. The obtained material was washed with water and dried in oven at 80 °C for 6 h. The final catalysts were denoted as Pt(X)@CMK-3 and Pt(X)@N-CMK-3 respectively, where X denotes Pt loading amount. In parallel, the preparation of the Pt/N-CMK-3 was achieved by impregnation procedure using N-CMK-3 as the support.

For comparison purpose, Pt/CNT@C was synthesized by a conventional impregnation method and hydrothermal coating process. Briefly, 1 g of purified CNT was suspended in 50 ml of deionized water containing a desired amount of H₂PtCl₆. After stirring for 4 h, the solvent was evaporated at 90 °C in a water bath. Then the resulting powder was calcined at 500 °C for 5 h in N₂ atmosphere, followed by reducing at 300 °C under H₂ atmosphere for 2 h. The coated catalyst precursor was obtained and denoted as Pt/CNT. To prepare coated catalyst by carbon shell, 1 g of the catalyst precursor and 4 g of glucose were added into 30 ml of deionized water, which were ultrasonically dispersed for 30 min. The mixture was transferred into a 50 ml of Teflon-lined stainless-steel autoclave for hydro-thermal treatment at 200 °C for 12 h. After cooling down to room temperature, the composite material was washed with deionized water and dried at 60 °C in a vacuum oven for 12 h. The material was further carbonized at 850 °C for 5 h with a ramping rate of 5 °C min⁻¹ under N₂ atmosphere. The resulting catalyst was denoted as Pt(X)/CNT@C, where X denotes Pt loading amount.

Catalyst characterization

The X-ray diffraction (XRD) was conducted on a Rigaku D/max-RA powder diffraction-meter using a Cu K_α radiation (Rigaku, Tokyo, Japan). Transmission

electron microscopy (TEM) images of the samples were collected on a JEM-200CX electron microscope (JEOL Co., Tokyo, Japan). The Pt contents of the catalysts were determined using an Inductive Coupled Plasma (ICP) Emission Spectrometer (J-A1100, Jarrell-Ash, USA). N₂ adsorption–desorption isotherms were conducted on a Micromeritics ASAP 2020 instrument (Micromeritics Instrument Co., Norcross, GA, USA) at –196 °C. Elemental analysis was conducted on an elemental analyzer (CHN-O-Rapid, Germany). EDS mapping and high-angle annular dark field (HAADF)-TEM were performed on an ARM-200F transmission electron microscope (JEOL Co., Japan.) with an X-MAX energy dispersive spectrometer (Oxford, UK). X-ray photo electron spectroscopy (XPS) was recorded on an ESCALAB250 (Thermo Scientific, USA) equipped with a monochromatized Al K α X-ray source ($h\nu=1486.6\text{eV}$). The binding energy values were calibrated using the C1s peak (284.8eV).

The points of zero charge (PZC) of the samples were determined using potentiometric mass titration method. Briefly, 0.1 g of the sample was added in 20 ml of 0.01 M NaCl solution at 25.0 °C, which was bubbled by a N₂ flow (50 ml min⁻¹). Then, 0.2 ml of 1.0 M NaOH solution was added to the suspension. After equilibration for 20 h, the catalyst suspension was titrated using a 0.5 M HCl solution, and the pH was monitored until constant. The blank solution (without catalyst) was also titrated following the same procedure.

The exposed Pt sites of the catalysts were determined by the CO chemisorption method. Briefly, a desired amount of catalyst was loaded in a U-shaped quartz tube and was activated in a H₂ stream (40 ml min⁻¹) at 300 °C for 2 h. After purging with an Ar flow (30 ml min⁻¹) at 300 °C for 1 h, the catalyst was cooled down to room temperature. The CO chemisorption was conducted using the pulse titration model and the CO contents in the pulses were monitored with a thermal conductivity detector.

Supplementary Figures (Figure S1 to Figure S13)

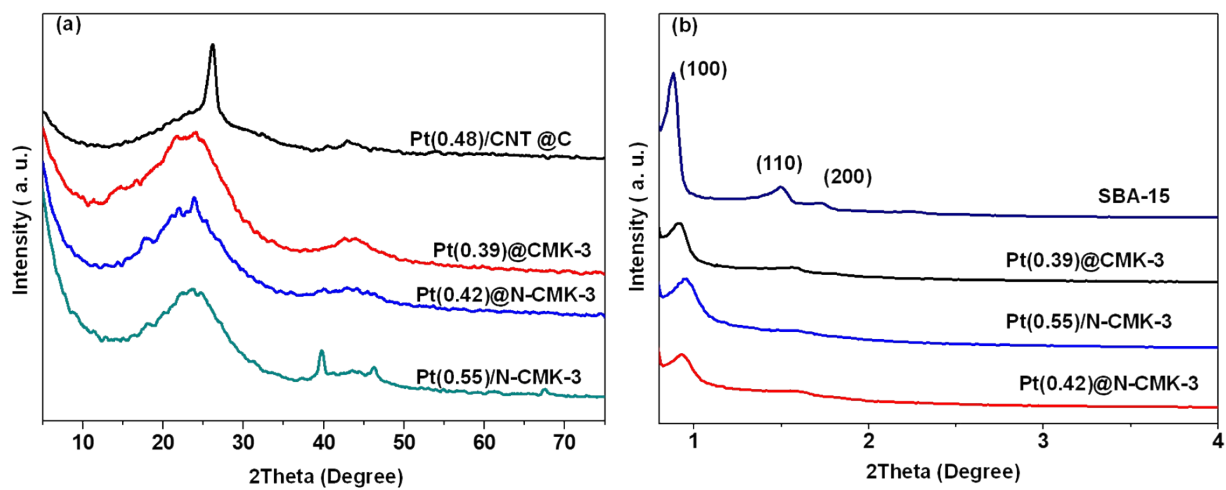


Fig. S1. (a) Wide and (b) small-angle XRD patterns of samples.

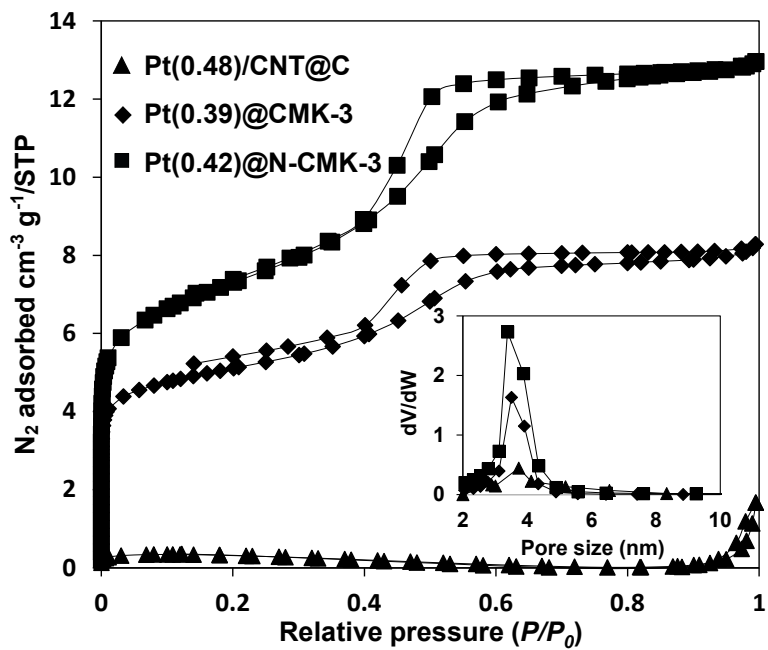


Fig. S2. N_2 adsorption-desorption isotherms and pore size distributions of Pt catalysts.

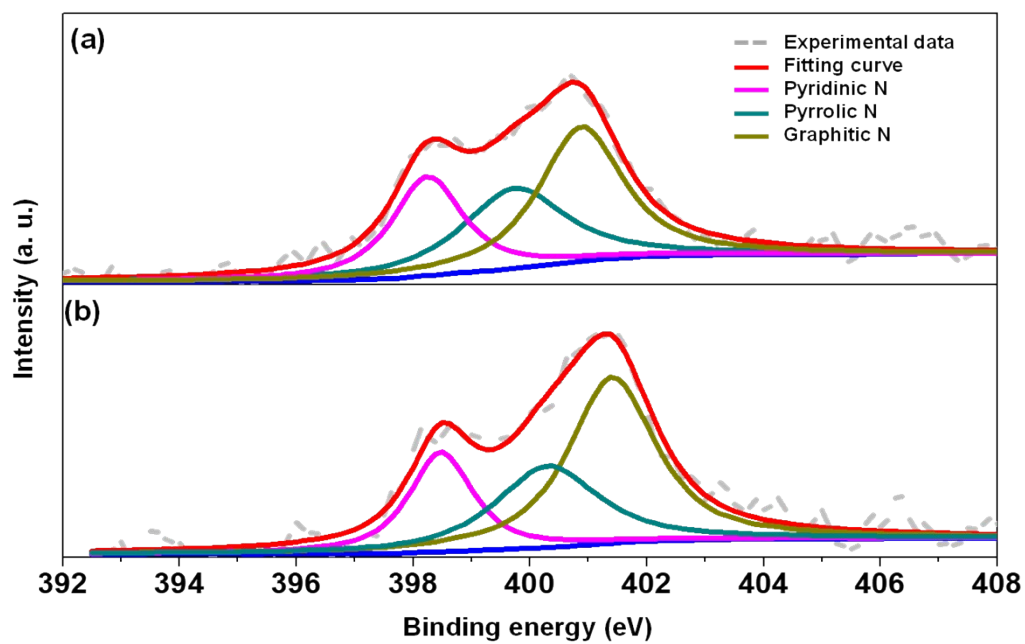


Fig. S3. XPS spectra of (a) Pt(0.55)/N-CMK-3 and (b) Pt(0.42)@N-CMK-3 in the N1s region.

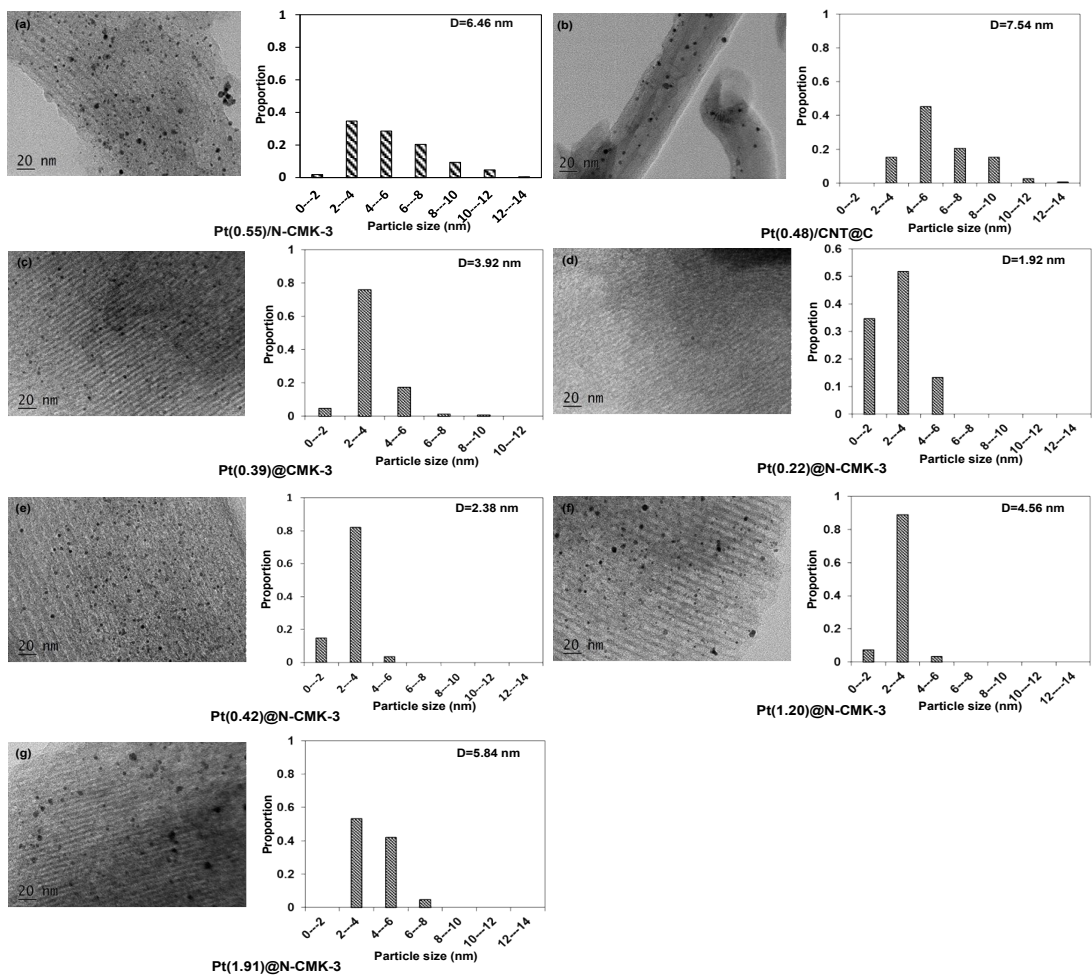


Fig. S4. TEM images of Pt catalysts and distribution histograms of the Pt particles.

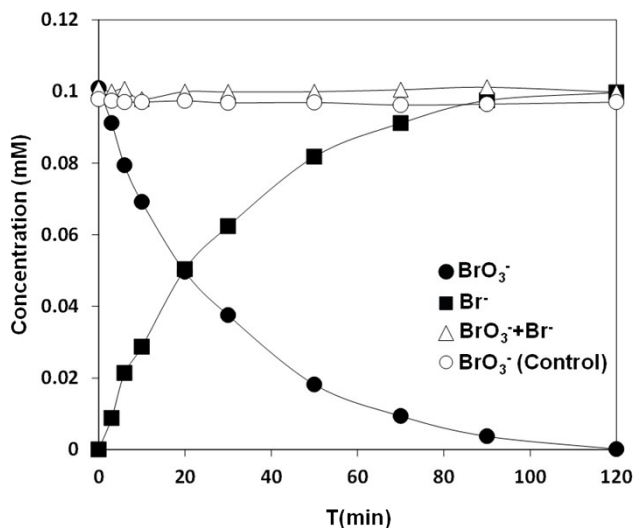


Fig. S6. Control experiment on N-CMK-3 and mass balance of catalytic hydrogenation reduction of bromate on Pt(0.42)@N-CMK-3. Reaction conditions: 0.1 mM bromate, 200 ml min⁻¹ H₂ flow and 0.1 g l⁻¹ catalyst at pH=5.6.

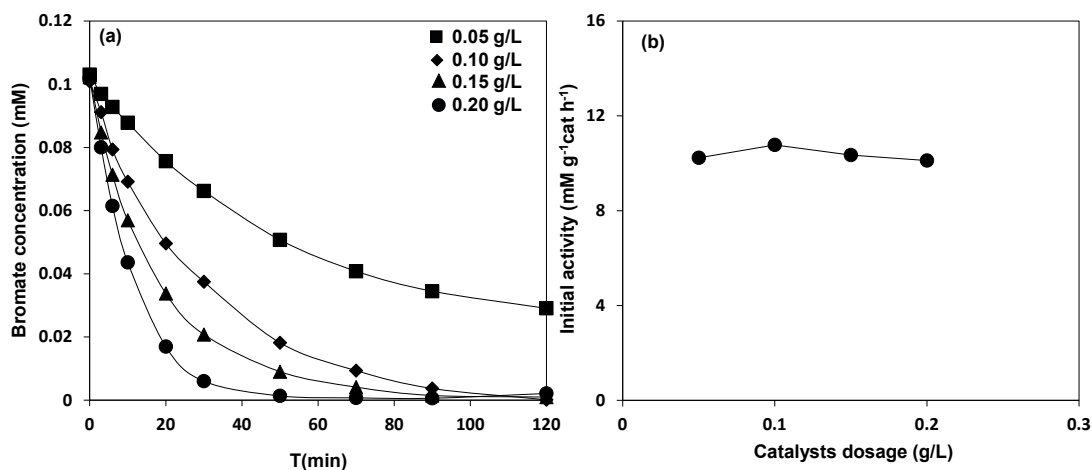


Fig. S7. (a) Catalytic hydrogenation reduction of bromate on Pt(0.42)@N-CMK-3 with varied catalyst dosages and (b) influence of catalyst dosage on the initial activity (r_0) of catalyst. Reaction conditions: 0.1 mM bromate and 200 ml min⁻¹ H₂ flow at pH=5.6. It was found that the initial activities normalized by catalyst dosage were nearly constant. The results excluded the influence of mass transfer limitation under the experimental conditions.^{9,10}

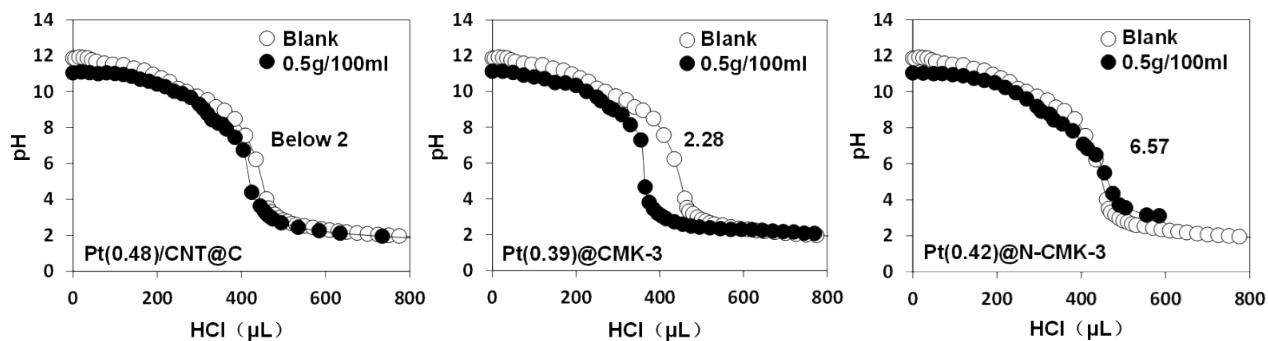


Fig. S8. Point of zero charge (PZC) titration curves of the catalysts.

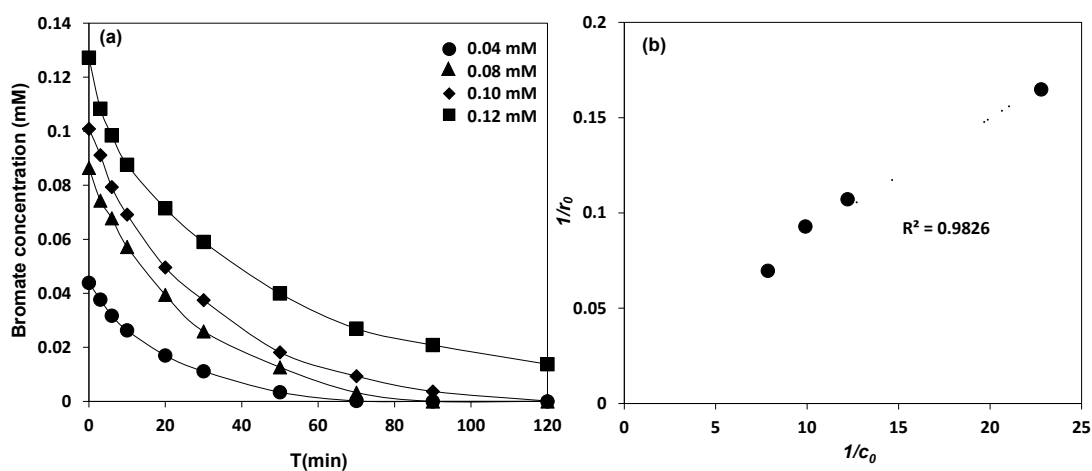


Fig. S9. (a) Influence of initial bromate concentration on bromate reduction over Pt(0.42)/@N-CMK-3 and (b) linear plot of $1/r_0$ versus $1/C_0$. Reaction conditions: 200 ml min^{-1} H_2 flow and 0.1 g l^{-1} catalyst at $\text{pH}=5.6$. The initial catalytic activity of Pt(0.42)/@N-CMK-3 increased from 6.07 to 14.39 $\text{mMgCat}^{-1}\text{h}^{-1}$ with the increase of initial bromate concentration from 0.04 to 0.12 mM, suggesting that reactant adsorption enhanced reaction activity (Fig. S9(a)). The reaction data were fitted to the Langmuir-Hinshelwood model, which was described as follows:¹¹

$$r_0 = k\theta_s = k \frac{bC_0}{1+bC_0} \quad (1)$$

$$\frac{1}{r_0} = \frac{1}{kC_0} + \frac{1}{k} \quad (2)$$

where r_0 is the initial reduction rate at bromate concentration of C_0 , θ_s is the coverage of bromate adsorption on the catalyst surface, k is the reaction rate constant,

and b is the equilibrium constant for bromate adsorption. The plot of $1/r_0$ versus $1/C_0$ is presented in Fig. S9(b) and a good linear relationship between $1/r_0$ and $1/C_0$ was obtained with $R^2 = 0.98 > 0.96$. The well described results by the Langmuir–Hinshelwood model indicated that bromate catalytic conversion was controlled by the adsorbed bromate on catalyst surface the rate controlling step, confirming the importance of bromate adsorption on catalytic activity.

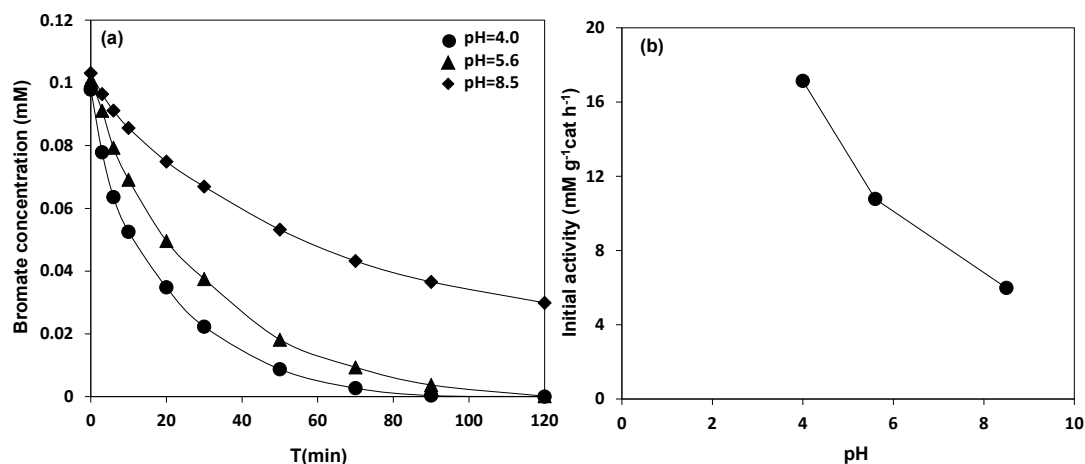


Fig. S10. (a) Influence of pH on the catalytic reduction of bromate on Pt(0.42)@N-CMK-3 and (b) dependence of initial rate on pH. Reaction conditions: 0.1mM bromate, 200 ml min⁻¹ H₂ flow and 0.1 g l⁻¹ catalyst. With the decrease of pH from 8.5 to 4.0, the initial catalytic activity of Pt(0.42)@N-CMK-3 increased from 6.0 to 17.1 mMgCat⁻¹h⁻¹, displaying a reverse relationship between catalytic bromate reduction and pH. The PZC of the Pt@N-CMK-3 was determined to be 6.57. Therefore, at pH below 6.57, the positively charged catalyst surface enhanced adsorption of bromate via electrostatic attractive interaction and thus increased bromate reduction due to protonation effects. On the contrary, at high pH, deprotonation of shell surface functionalities resulted in negatively charged catalyst surface, which invoked electrostatic repulsive interaction with bromate, giving rise to suppressed bromate adsorption and catalytic conversion.^{12,13}

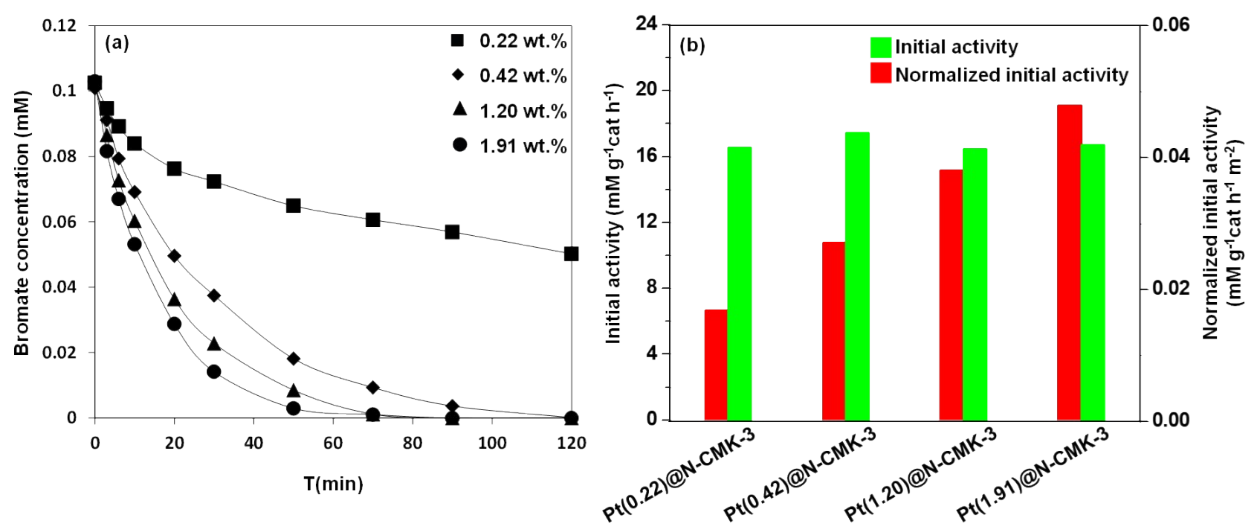


Fig. S11. (a) The catalytic reduction of bromate on Pt@N-CMK-3 catalysts with varied Pt loading amounts, (b) Normalized initial activity by interface areas of Pt-CN heterojunctions. The interface areas of Pt-CN were calculated to be 160.4, 245.8, 366.5, and 455.5 m² g⁻¹ for Pt(0.22)@N-CMK-3, Pt(0.42)@N-CMK-3, Pt(1.20)@N-CMK-3, and Pt(1.91)@N-CMK-3, respectively (see details in Calculation S2). Reaction conditions: 0.1 mM bromate, 200 ml min⁻¹ H₂ flow and 0.1 g l⁻¹ catalyst at pH=5.6.

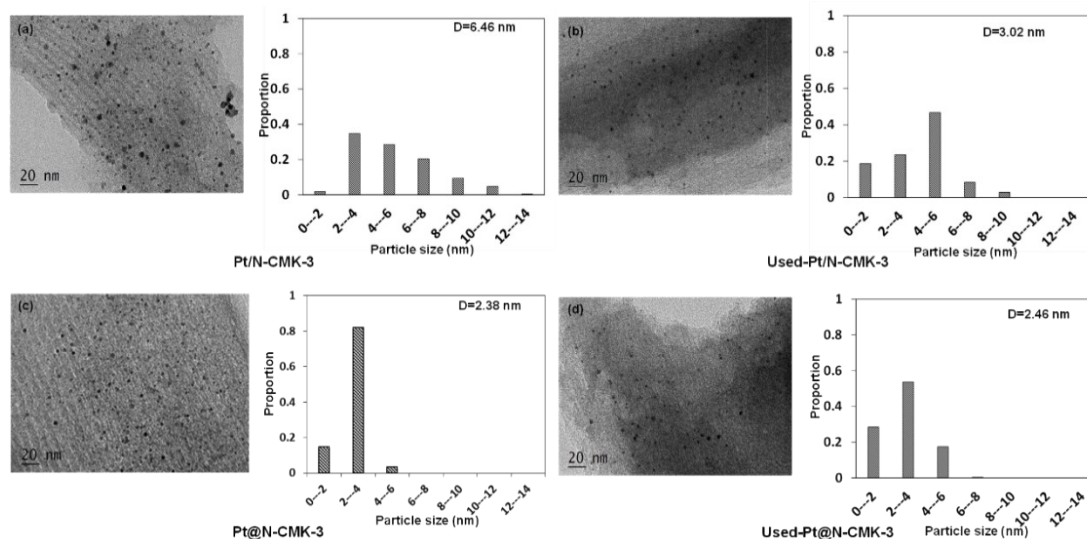


Fig. S12. TEM images and corresponding Pt particle size distributions of (a)Pt(0.55)/N-CMK-3, (b)used Pt(0.55)/N-CMK-3, (c) Pt(0.42)@N-CMK-3 and (d) used Pt(0.42)@N-CMK-3.

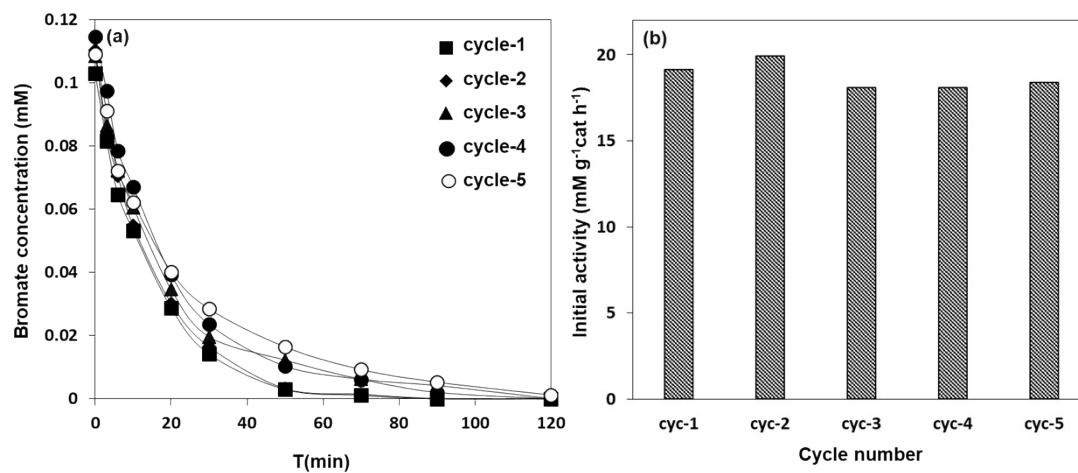


Fig. S13. The consecutive catalyst cycle of Pt(1.91)@N-CMK-3 (a) and the corresponding initial activities of catalyst in each reaction cycle (b). Reaction condition: 0.1 mM bromate, 200 ml min⁻¹ H₂ flow and 0.1 g l⁻¹ catalyst at pH=5.6.

Supplementary Table

Table S1 Physicochemical properties of the catalysts.

sample	Pt Content (wt. %) ^a	Particle size (nm) ^b	S _{BET} (m ² /g) ^c	V _t (cm ³ /g) ^c	W _{BJH} (nm) ^c	N content (%)	CO chemisorption (μmol g ⁻¹)
Pt(0.48)/CNT@C	0.48	7.54	16.3	0.02	4.10	BDL ^e	BDL ^e
Pt(0.55)/N-CMK-3	0.55	6.46	733.4	0.80	4.92	0.114	17.6
Pt(0.39)@CMK-3	0.39	3.92	378.9	0.28	2.95	BDL ^e	BDL ^e
Pt(0.22)@N-CMK-3	0.22	1.92	908.3	0.96	3.98	0.121	BDL ^e
Pt(0.42)@N-CMK-3	0.42	2.38	699.0	0.75	4.28	0.107	BDL ^e
Pt(1.20)@N-CMK-3	1.20	4.56	697.9	0.54	3.32	0.098	BDL ^e
Pt(1.91)@N-CMK-3	1.91	5.84	606.2	0.47	3.36	0.110	0.001

^a Determined by ICP-AES.

^b calculated in the basis of TEM images.

^c Deduced from the isotherm analysis.

^d Not detected.

^e Below detection limit.

Table S2 Comparison of catalytic bromate reduction on Pt@N-CMK-3 with some noble metal catalysts reported in literature.

Catalyst	pH	Metal loading (wt.%)	Initial activity (mMgCat⁻¹h⁻¹)	Reference
Pt@N-CMK-3	5.6	0.42	10.8	This work
Pd/Al ₂ O ₃	5.6	1.93	10.7	[16]
Pt/AC	5.5	1.0	0.7	[17]
Ir/AC	5.5	1.0	0.5	
Ru/AC	5.5	1.0	1.6	
Rh/AC	5.5	1.0	1.4	
Pd/MCN	5.6	2.2	40.0	[18]
CuPd-ZSM-5	neutral	0.55(Cu)/1.90(Pd)	2.6	[19]
Pd(0.1)/Fe ₃ O ₄	neutral	0.1	5.9	[20]

Calculation S1

The average sizes of Pd particles in the catalysts were estimated based on surface area weighted diameter: ^{14,15}

$$\bar{d}_s = \sum n_i d_i^3 / \sum n_i d_i^2$$

Where n_i is the counting number of Pd particles with diameter of d_i and the total number ($\sum n_i$) exceeds 100. The values of d_i and n_i were obtained from the TEM images.

Calculation S2

The interface areas of Pt-CN heterojunctions in the catalysts were calculated as the following equation:

$$S_{Pt-CN} = 4\pi r^2 \times \frac{m_{Pt}}{\rho \times \frac{4}{3}\pi r^3}$$

Where S_{Pt-CN} ($\text{m}^2 \text{g}^{-1}$) is the total interface area of Pt-CN, r (m) is obtained from TEM observation assuming a spherical shape of Pt nanoparticle with an average radius. A Pt loading amount m_{Pt} is determined by ICP-AES. ρ (g m^{-3}) is the density of Pt particles

and $\frac{4}{3}\pi r^3$ is the volume of single Pt particle with average radius of r .

References

1. C. G. Hu, Z. Y. Bai, L. Yang, J. Lv, K. Wang, Y. M. Guo, Y. X. Cao, J. G. Zhou, *Electrochim. Acta* 2010, **55**, 6036–6041.
2. K. Jukk, N. Alexeyeva, C. Johans, K. Kontturi, K. Tammeveski, *J. Electroanal. Chem.*, 2012, **666**, 67–75.
3. D. Y. Zhao, J. L. Feng, Q. S. Huo, N. Melloh, G. H. Fredrickson, B. F. Chmelka, G. D. Stucky, *Science*, 1998, **279**, 548–552.
4. S. H. Joo, S. J. Choi, I. Oh, J. Kwak, Z. Liu, O. Terasaki, R. Ryoo, *Nature*, 2001, **412**, 169.
5. M. Kruk, M. Jaroniec, T. W. Kim, R. Ryoo, *Chem. Mater.*, **2003**, 15, 2815–2823.
6. G. Blanco, J. M. Pintado, K. Aboussaïd, G. A. Cifredo, M. S. Begrani, S. Bernal, *Catalysis Today*, 2012, **180**, 184–189.
7. M. Lo'pez-Haro, K. Aboussaïd, J. C. Gonzalez, J. C. Herna'ndez, J. M. Pintado, G. Blanco, J. J. Calvino, P. A. Midgley, P. Bayle-Guillemaud, S. Trasobares, *Chem. Mater.*, 2009, **21**, 1035–1045.
8. A. H. Lu, W. C. Li, W. Schmidt, W. Kiefer, F. Schüth, *Carbon*, 2004, **42**, 2939–2948.
9. G. Yuan, M.A. Keane, *Chem. Eng. Sci.*, 2003, **58**, 257–267.
10. O. M. Ilinitich, F. Petrus Cuperus, L. V. Nosova, E. N. Gribov, *Catal. Today*, 2000, **56**, 137–145.
11. A. Pintar, J. Batista, J. Levec, T. Kajiuchi, *Appl. Catal. B: Environ.*, 1996, **11**, 81–98.
12. G. Yuan, M. A. Keane, *Ind. Eng. Chem. Res.*, 2007, **46**, 705–715.
13. S. Gomez-Quero, F. Cardenas-Lizana, M. A. Keane, *Ind. Eng. Chem. Res.*, 2008, **47**, 6841–6853.
14. C. Amorim, G. Yuan, P. M. Patterson, M. A. Keane, *J. Catal.*, 2005, **234**, 268–281.
15. G. Yuan, M. A. Keane, *Appl. Catal. B Environ.*, 2004, **52**, 301–314.
16. H. Chen, Z.Y. Xu, H.Q. Wan, J.Z. Zheng, D.Q. Yin and S.R. Zheng, *Appl. Catal. B- Environ.*, 2010, **96**, 307.

17. J. Restivo, O.S.G.P. Soares, J.J.M. Órfão and M.F.R. Pereira, *Chem. Eng. J.*, 2015, **263**, 119.
18. P. Zhang, F. Jiang and H. Chen, *Chem. Eng. J.*, 2013, **234**, 195.
19. C.M.A.S. Freitas, O.S.G.P. Soares, J.J.M. Órfão, A.M. Fonseca, M.F.R. Pereira and I.C. Neves, *Green Chem.*, 2015, **17**, 4247.
20. W.H. Sun, Q. Li, S.A. Gao, J.K. Shang, *J. Mater. Chem. A*, 2013, **1**, 9215–9224.